Published in final edited form as:
Neurosurg Focus. 2009 July ; 27(1): E9. doi:10.3171/2009.4.FOCUS0974.

Human neocortical electrical activity recorded on nonpenetrating microwire arrays: applicability for neuroprostheses

Spencer S. Kellis, B.S.[1,*], **Paul A. House, M.D.**[2], **Kyle E. Thomson, M.S.**[3], **Richard Brown, Ph.D.**[1], and **Bradley Greger, Ph.D.**[3]

[1] Department of Electrical and Computer Engineering, University of Utah, Salt Lake City, Utah

[2] Department of Neurosurgery, University of Utah, Salt Lake City, Utah

[3] Department of Bioengineering, University of Utah, Salt Lake City, Utah

Abstract

Object—The goal of this study was to determine whether a nonpenetrating, high-density microwire array could provide sufficient information to serve as the interface for decoding motor cortical signals.

Methods—Arrays of nonpenetrating microwires were implanted over the human motor cortex in 2 patients. The patients performed directed stereotypical reaching movements in 2 directions. The resulting data were used to determine whether the reach direction could be distinguished through a frequency power analysis.

Results—Correlation analysis revealed decreasing signal correlation with distance. The gamma-band power during motor planning allowed binary classification of gross directionality in the reaching movements. The degree of power change was correlated to the underlying gyral pattern.

Conclusions—The nonpenetrating microwire platform showed good potential for allowing differentiated signals to be recorded with high spatial fidelity without cortical penetration.

Keywords

human; motor cortex; electrocorticoencephalography; neuroprosthesis

Various approaches have been used successfully to correlate neuronal activity with specific movements. In some cases, this correlation has been device or cursor.[5,8] Approaches based on standard ECoG electrode arrays, used in most of the studies involving human subjects, have required the user of the device to focus on movement of different body parts. This requires participants to use nonintuitive movements to control an external device. It is possible that such nonintuitive control signals have been required because of the limited spatial fidelity of the physical interface with the neocortex that is provided by ECoG electrodes.

The most successful applications allowing for the direct control of an external device based on the normal neuronal patterns produced during spontaneous movement have used the firing patterns of multiple single neurons in primates.[6,9,11,14] Such decoding is technically

Address correspondence to: Paul A. House, M.D., Department of Neurosurgery, University of Utah, Salt Lake City, Utah. neuropub@hsc.utah.edu.
*Spencer S. Kellis and Dr. Paul A. House contributed equally to this study.

Disclosure
Support for this study was provided by DARPA BAA05-26 Revolutionizing Prosthetics and by the Engineering Research Center Program of the National Science Foundation under award EEC-9986866.

challenging, requiring sophisticated action potential identification and sometimes long and repeated training sessions in addition to direct implantation of microelectrodes into the neocortex. Even with these noted limitations, however, these techniques have been successfully used in humans.[3,4]

Penetrating microelectrode arrays currently have maximum in vivo lifetimes of only a few years. Although some successful long-term recordings have been obtained with penetrating cortical arrays, a loss of action potential signal quality over time has also been observed.[10] Additionally, penetrating microwire assemblies in place over the long term can have difficulty maintaining recordings from an individual neuron, probably because of micro-motion of the device relative to the neural tissue.

These drawbacks have provided an impetus to investigate whether other platforms might allow for less invasion into the neocortex while still providing more spatial and temporal resolution than is currently possible with electroencephalography or standard ECoG grids. Non-penetrating microwire arrays are one such platform that has recently been reported.[13] These arrays have different physical properties—such as higher electrical impedances—than standard ECoG recording electrodes, yet are not as closely approximated to the neural tissue as are penetrating microelectrodes. These electrical properties require different amplification and signal analysis capabilities than those available with clinical electroencephalography recording equipment, limiting investigations using nonpenetrating microwires to research protocols.[15] Here, we describe preliminary investigations using a nonpenetrating microwire platform to derive local neuronal signals and determine whether these signals contain sufficient information to differentiate directionality of a relatively stereotyped movement.

Methods

Two male patients who required extraoperative electrocorticographic monitoring for medically refractory epilepsy were enrolled in an institutional review board–approved protocol. Informed consent was obtained from each patient.

The first patient (Case 1) was implanted with two 16-channel nonpenetrating microwire arrays (40-μm wire; PMT Corporation) with 1-mm interelectrode spacing, placed in the epipial space underneath a standard clinical ECoG grid (Fig. 1). This patient suffered primarily from complex partial seizures subsequently shown to originate in the posterior left temporal area. He harbored significant occipital encephalomalacia from a perinatal injury, but the perirolandic area where the arrays were placed was essentially normal on MR imaging. One of the arrays was placed over the upper extremity primary motor cortex as confirmed on intraoperative somatosensory evoked potential monitoring. The other array was placed more inferiorly along the precentral gyrus. Both arrays were referenced to a pair of epidural bare wires.

The second patient (Case 2) underwent implantation of a single 30-channel nonpenetrating microwire array with 2-mm interelectrode spacing. This patient harbored a large right parietal gliotic cyst abutting the postcentral gyrus and suffered from focal motor and complex partial seizures. The anterior portion of the array was placed over the hand area of the primary motor cortex as confirmed on extraoperative electrical stimulation with electromyographic confirmation. The array was referenced to 2 low-impedance electrodes built into the device. A standard ECoG grid with 1-cm electrode spacing was also placed on top of the array.

After electrode placement, the patients underwent observation in the Neurocritical Care Unit for continuous seizure monitoring. The first patient was monitored for 2 weeks and performed 7 sets of movement tasks; the second patient was monitored for 5 days and performed 3 sets of movement tasks.

Motor Tasks

The patients were instructed to perform simple, repetitive movements using a computer mouse. The mouse position was recorded continuously with a computerized pen tablet (Wacom Co., Ltd.). Movement was accomplished using the hand and arm contralateral to the hemisphere in which the ECoG electrode array and non-penetrating microwire array were located. On verbal cue, the patient moved the mouse from a starting position at the bottom center of the tablet to the upper left or the upper right corner, and then returned the mouse to the start position.

The order of targets was determined beforehand to be interleaved pseudorandomly and was communicated through the verbal cue. Trials lasted 2–3 seconds with 1-second separation. Only trials at least 80% within 1 SD of the average path in both the horizontal and vertical components of movement were retained for analysis. Approximately 20–30 recorded trials per patient per modality of movement remained after filtering. Plots of the recorded and analyzed movements and velocities for a portion of 1 patient recording are shown in Fig. 2.

The tablet and array outputs were recorded with a NeuroPort system (Blackrock Microsystems). During digitization, the signals were band-pass filtered to preserve frequencies between 0.3 Hz and 7.5 KHz. Electrode data were recorded at 30,000 samples/second, and movement data were recorded at either 2000 samples/second or 30,000 samples/second. All movement and electrode data were recorded with the same sampling and filtering process simultaneously, ensuring that the movement position was well synchronized to ECoG data.

Correlation Analysis

Pairwise cross-correlation analysis between each set of nonpenetrating microwires was performed on neuronal recordings from a period during arm movement to explore the strength of the linear relationship between the signals recorded by nonpenetrating microwires nearby. Because the correlation metric indicates the degree to which 2 sequences are linearly related, this estimation of independence, while not a complete metric, can approximate the possible usefulness of the high spatial resolution recording afforded by the nonpenetrating microwire devices. In particular, the correlation analysis should help to clarify whether the nonpenetrating microwire array could be replaced by a single large electrode, or if the tighter spacing of the nonpenetrating microwires allows for recording of potentially unique signals.

Neural data were band-pass filtered to 30–80 Hz. For each movement trial, one second of filtered data was used to generate pairwise correlation coefficients for each combination of channels. For each pair of channels, the resulting correlation coefficients were averaged, with results presented visually in Fig. 3.

Signal Analysis

Raw neural data were first downsampled from 30,000 samples/second to 3000 samples/second. To adaptively mitigate the effects of 60-Hz noise, the trial-averaged spectrum for each nonpenetrating microwire was calculated to determine the width and amplitude of the 60-Hz noise band. Across all nonpenetrating microwires in the second patient, for example, noise levels in this band ranged 5–20 dB above the normal spectrum, meaning that a single filter might effectively attenuate noise in a few channels but would leave large banding in most of the data. Therefore, a fifth-order Chebyshev Type-II filter was designed to individually mirror the calculated width and height of the 60-Hz noise. Next, the data were filtered to remove frequencies below 5 and above 150 Hz using fifth-order Butterworth filters. In general, all filtering was performed with commercially available software (Matlab, The MathWorks), running once in the forward and once in the reverse direction, with appropriate initial conditions in the second pass, to ensure zero phase distortion.

Trial components were marked by points where the velocity of the patient's motion crossed a threshold of 1 SD from rest. This model was used to mark both outward and return movement; additionally, baseline trials were marked at periods of no movement between trials. Only outward movement trials were included in the present analysis. The timestamps of these outward movements were used as markers for reading electrode data. For spectrograms we used 1-second windows with movement aligned at 0.5 seconds.

Spectrograms were generated using the open-source Chronux package software (chronux.org) with 250-msec windows and 50-msec step size; tapering parameters were set to a time-bandwidth product of 5 and 9 leading tapers. Spectrum plots of the raw data were characterized by a power law trend whose features dominated frequency analysis. For this reason, the spectrograms were normalized to the trial-averaged spectrum for all trials of like movement.

Differential power analysis was performed by normalizing the average gamma-band power between movements in the contralateral and ipsilateral directions to the average power in spectrograms from just contralaterally directed movement. First, spectrograms were generated in the same manner described above for data from each microwire. Next, the power in the region between 30 and 80 Hz for times between −500 and 0 msec was averaged to a single value. Once these averaged powers were obtained for each nonpenetrating microwire (independently calculated for each direction of movement), the values for the contralateral direction were rereferenced against the ipsilateral values, then normalized by division to the contralateral values. In this way, the percent change of gamma-band power between contralateral and ipsilateral directions of movement was obtained for each channel in the nonpenetrating microwire array.

Results

No difficulties such as hemorrhage or electrode migration were encountered during placement, use, or removal of the nonpenetrating microwire arrays. The motor task design was designed to be simple in nature so that patients could participate in trials even on the first postoperative day after array implantation.

As noted previously, microwires have significantly higher electrical impedance characteristics than standard ECoG electrodes. However, the recording system used was originally designed for single-unit action potential analysis from penetrating high-impendance sources. This US Food and Drug Administration–approved system handled signals from the nonpenetrating microwire arrays as well as the standard ECoG contacts without modification of the amplification system.

Correlation Analysis

Figure 3 shows the correlation coefficients mapped to each electrode for all devices placed in both patients. The first patient showed a decrease in correlation with distance. The patient in Case 2 had an area of high correlation on the anterior side of the device. The posterior half of the array showed a drop-off similar to that seen in both arrays placed in the first patient. The correlation between nonpenetrating microwires in the first patient ranged between 50 and 100%; for the second patient the range was 0–100%. For both patients, a stronger correlation was generally found between closer nonpenetrating microwires. The decay in correlation strength over distance indicates a degree of independence present across the array; that is, the nonpenetrating microwire array did not act as a single macroelectrode. Additionally, the disparity between correlations in the anterior and posterior regions in Case 2 is supported by the underlying anatomy. The highly correlated anterior portion in the patient in Case 2 is directly over the hand area in primary motor cortex.

Movement Analysis

The patients were able to participate in the motor tasks without significant difficulty. The majority of movements were relatively stereotyped, and only movements within an SD of the average path were used. As the recording properties of the nonpenetrating microwire system were not well known, signals were initially visually evaluated using a limited frequency range (0–70 Hz). Visual inspection revealed ECoG-like recordings in which some standard features such as interictal spikes could be identified.

Spectrograms were created for each patient by averaging results from a single reaching task session. Visual analysis of the spectrograms revealed significant and consistent patterning consistent with previous analyses, including modulation in the beta band power before and during movement.[12] Although data from only a single nonpenetrating microwire are displayed in Fig. 4, these results are representative of data from most microwires in both patients (Figs. 5 and 6 show spectrograms generated over all arrays). In general, a substantial increase in gamma-band power was noted to occur before movement onset in the contralateral direction, with much less gamma-band power seen related to movement in the ipsilateral direction.

Modulation of power in the lower gamma band was especially noticeable in the first patient, with activity evident around 30–40 Hz beginning 500 msec before movement in the contralateral direction and quickly dropping off after onset of movement. The corresponding region for ipsilaterally directed tasks in this patient was relatively devoid of similar activity, showing instead a general attenuation in power over the entire gamma band. Power modulation was also evident across the entire gamma band in the second patient.

Because of the simple design of the reaching task, the outward reach movement was immediately followed by the return movement. Gamma-band activity, while generally increased prior to movement, was evident during the outward reaching movement. We presume that this increased activity is representative of planning for the return movement. For example, in Fig. 4, Case 2 ipsilateral (−0.1 sec, 75–100 Hz), the upper gamma-band power increases significantly during outward movement. This increase in power occurs ~ 500 msec before initiation of the return movement. Similar activity is evident, albeit to a lesser degree, in the second patient during planning for the outward movement.

Figure 7 shows the percent change in average gamma-band power during planning for movement in the contralateral versus the ipsilateral direction for 500 msec preceding movement. The difference between these mean values was reasonably substantial. This metric revealed patterns consistent with the underlying anatomy. For example, in the first patient, channels 17–32 were placed over the upper extremity primary motor cortex as confirmed intraoperatively with phase reversal of the somatosensory evoked potential signals. We attempted to place these channels over the expected hand area, with channels 1–16 being placed closer to the expected face area. Channels 17–32 showed significantly higher directional preference as indicated by a 20–30% increase in signal power over 14 of 16 microwires when direction of movement changed from ipsilateral to contralateral targets. Channels 1–16 showed very small gains of < 10%. In the patient in Case 2, extraoperative stimulation confirmed that the majority of the array was over the primary hand motor cortex with the higher numbered contacts lying over the post-central gyrus. Gamma band power increases followed the gyral contours, with nonpenetrating microwires known to record over hand area indicating a 40–60% change in power for movement in the contralateral direction. Microwires over the parietal cortex recorded slightly lower changes in power (30–40%), whereas microwires over the rolandic vein recorded the lowest changes (around 20%).

Perhaps most interesting, however, is the level of detail evident in gradients in the percent change visible across both arrays. With only 1 or 2 mm of spacing between contacts, an entire

nonpenetrating microwire array fits into the area covered by 1 or 2 standard ECoG electrodes. Individual microwire contacts are clearly recording activity not fully present in other channels in the array. These results suggest that binary classification between movements in grossly contralateral or ipsilateral directions is possible using microwires spaced millimeters apart.

Discussion

We designed this study to investigate whether a nonpenetrating microwire device can serve as a brain-machine interface for a motor neural prosthesis. We wished to determine whether these nonpenetrating microwires could acquire neural information potentially useful for decoding motor intentions. Given the known size of the human primary motor hand cortex, the grid was designed to allow for decoding of individual finger and hand movements. As a first assessment, we examined the larger and more easily measured arm movements.

As might be expected from the small size of these devices and the gross motor task chosen, a high degree of interelectrode correlation was found. One would expect that, as interelectrode distance increases, the amount of correlation between the signals decreases. Our correlation analysis supported this assumption, with nonpenetrating microwires 1 cm apart having little correlation, whereas those placed 1 mm apart were nearly 90% correlated in the 30–80 Hz frequency ranges. Although the results from this correlation analysis can help direct future array design, the requirements for a brain-machine interface device must also be considered.

It is likely that there is significant motor information represented at the scale of single cortical columns, and possible that a nonpenetrating microwire grid may be capable of acquiring “local field potential-like” signals at this scale. Extracting neural information at this spatial scale may be necessary to provide dexterous intuitive control of a prosthesis. At one extreme, accurate control for fine movements of an external device might require wires with subcolumnar spacing (< 100 μm). Such a system could then mimic the level and quality of neural information extracted with penetrating microelectrodes, other than recording action potentials. At another extreme, it is possible that nonpenetrating wires could only accurately measure an “ECoG-like” integrated signal from a broad region of cortex. If the information content available at the pial surface is substantially spatially limited, perhaps to a range of several millimeters, then the best motor decode possible using a nonpenetrating microwire system may not substantially differ from what is possible with a conventional ECoG grid or possibly epidural electrodes.

Our results indicate that signal variation can be found even across a spacing of 1–2 mm. This variance in motor neuronal signal pattern differentially noted during a simple reaching task shows that discrete information is being identified. The differential between small-scale signals might be useable for a motor decode.[1]

Tuning curves for directional preference of motor cortex cells have been extensively demonstrated in both single-unit action potential and also local field potential analysis from penetrating electrodes.[7,9] It is unknown whether such selectivity will be able to be demonstrated from the neuronal activity derived from nonpenetrating microwires given the discrete size of tuned cortical columns.[2] The data from this study suggest that at least a binary classification is possible between 2 directions, encouraging future studies to define the content of the neuronal signals being recorded more fully.

Conclusions

The primary finding of this study is that a nonpenetrating microwire platform allows the recording of human neocortical neuronal activity with spatial resolution better than that available with standard ECoG grids. We found the signals recorded from a nonpenetrating microwire array placed over the human motor cortex contained sufficient information so that

discrimination in gross direction could be identified during a simple motor task in the gamma-band frequency range. These results suggest that nonpenetrating microwire grids could serve as a recording platform for providing neural control over a motor prosthesis. However, more detailed studies of the nonpenetrating microwire arrays using both hand and arm movement tasks, and more sophisticated motor decode paradigms will be needed to validate applications of these grids. Nonpenetrating microwire grids may have greater longevity than penetrating microelectrode arrays, and we are conducting ongoing animal investigations to verify this theory.

By providing high spatial resolution electrophysiological recordings of human neocortical activity, nonpenetrating microwire arrays may be able to serve as an interface that provides dexterous intuitive control of a limb prosthesis. Additionally, this technology may serve as a novel research tool for studying spatially local neocortical phenomena in health and disease.

Acknowledgments

The authors thank Kristin Kraus, M.Sc., for editorial assistance preparing this paper. The authors also thank Renee Harrell for assistance with data collection, and Renee Thor, and the University of Utah EEG technicians for their help. The authors also acknowledge PMT, Inc., and Blackrock Microsystems for their technical support.

Abbreviation used in this paper

ECoG	electrocorticoencephalographic

References

1. Brunner C, Scherer R, Graimann B, Supp G, Pfurtscheller G. Online control of a brain-computer interface using phase synchronization. IEEE Trans Biomed Eng 2006;53:2501–2506. [PubMed: 17153207]
2. Georgopoulos AP, Merchant H, Naselaris T, Amirikian B. Mapping of the preferred direction in the motor cortex. Proc Natl Acad Sci U S A 2007;104:11068–11072. [PubMed: 17569784]
3. Hochberg LR, Serruya MD, Friehs GM, Mukand JA, Saleh M, Caplan AH, et al. Neuronal ensemble control of prosthetic devices by a human with tetraplegia. Nature 2006;442:164–171. [PubMed: 16838014]
4. Kennedy PR, Bakay RA, Moore MM, Adams K, Goldwaithe J. Direct control of a computer from the human central nervous system. IEEE Trans Rehabil Eng 2000;8:198–202. [PubMed: 10896186]
5. Leuthardt EC, Schalk G, Wolpaw JR, Ojemann JG, Moran DW. A brain-computer interface using electrocorticographic signals in humans. J Neural Eng 2004;1:63–71. [PubMed: 15876624]
6. Musallam S, Corneil BD, Greger B, Scherberger H, Andersen RA. Cognitive control signals for neural prosthetics. Science 2004;305:258–262. [PubMed: 15247483]
7. Rickert J, Oliveira SC, Vaadia E, Aertsen A, Rotter S, Mehring C. Encoding of movement direction in different frequency ranges of motor cortical local field potentials. J Neurosci 2005;25:8815–8824. [PubMed: 16192371]
8. Schalk G, Miller KJ, Anderson NR, Wilson JA, Smyth MD, Ojemann JG, et al. Two-dimensional movement control using electrocorticographic signals in humans. J Neural Eng 2008;5:75–84. [PubMed: 18310813]
9. Serruya MD, Hatsopoulos NG, Paninski L, Fellows MR, Donoghue JP. Instant neural control of a movement signal. Nature 2002;416:141–142. [PubMed: 11894084]
10. Suner S, Fellows MR, Vargas-Irwin C, Nakata GK, Donoghue JP. Reliability of signals from a chronically implanted, silicon-based electrode array in non-human primate primary motor cortex. IEEE Trans Neural Syst Rehabil Eng 2005;13:524–541. [PubMed: 16425835]
11. Taylor DM, Tillery SI, Schwartz AB. Direct cortical control of 3D neuroprosthetic devices. Science 2002;296:1829–1832. [PubMed: 12052948]

12. Uhlhaas PJ, Singer W. Neural synchrony in brain disorders: relevance for cognitive dysfunctions and pathophysiology. Neuron 2006;52:155–168. [PubMed: 17015233]

13. Van Gompel JJ, Stead SM, Giannini C, Meyer FB, Marsh WR, Fountain T, et al. Phase I trial: safety and feasibility of intracranial electroencephalography using hybrid subdural electrodes containing macro- and microelectrode arrays. Neurosurg Focus 2008;25(3):E23. [PubMed: 18759625]

14. Wessberg J, Stambaugh CR, Kralik JD, Beck PD, Laubach M, Chapin JK, et al. Real-time prediction of hand trajectory by ensembles of cortical neurons in primates. Nature 2000;408:361–365. [PubMed: 11099043]

15. Worrell GA, Gardner AB, Stead SM, Hu S, Goerss S, Cascino GJ, et al. High-frequency oscillations in human temporal lobe: simultaneous microwire and clinical macroelectrode recordings. Brain 2008;131:928–937. [PubMed: 18263625]

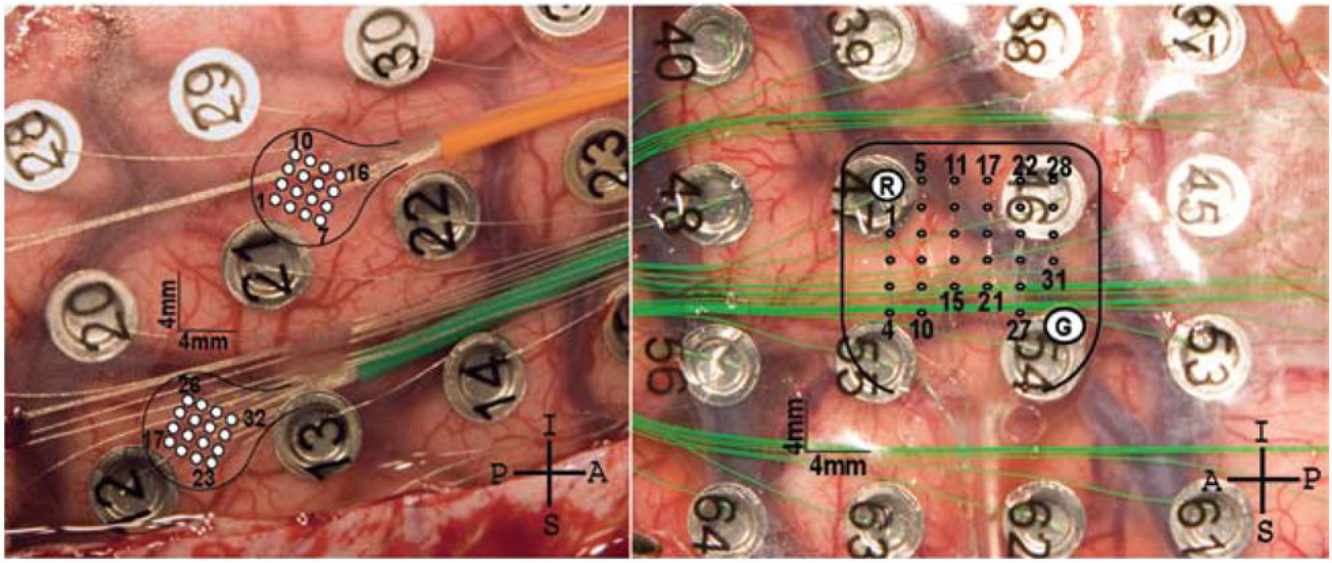

Fig. 1.

Photographs showing device implantation in the patients in Cases 1 and 2. *Left:* Two nonpenetrating microwire arrays (1-mm spacing) were implanted over the right primary motor cortex in the first patient. Channels 1–16 are over the hand area *(orange wire)*, and channels 17–32 are over the arm area *(green wire). Right:* A single 30-channel array (2-mm spacing) was implanted over the left primary motor cortex hand and arm area in the second patient.

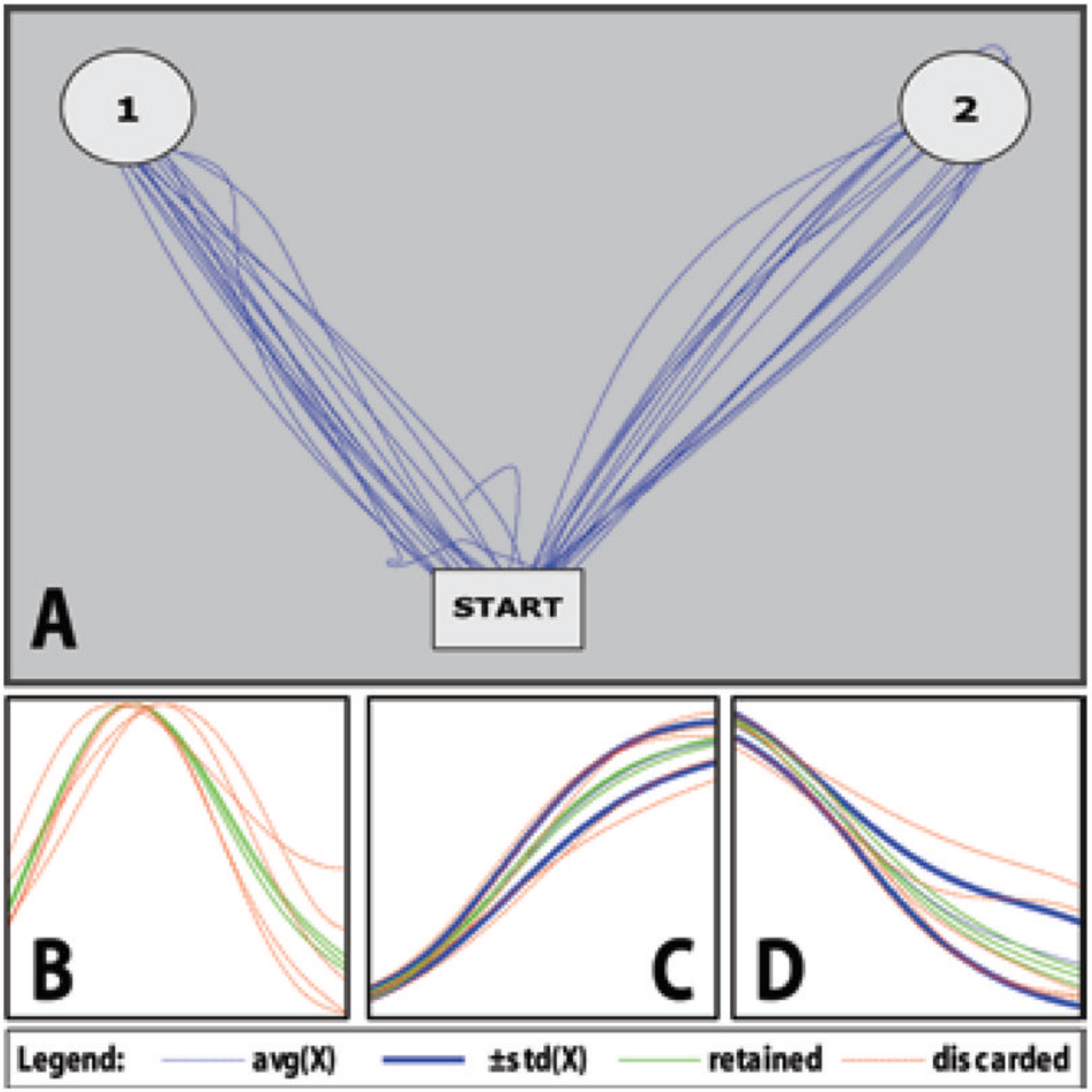

Fig. 2.

Trial detection and filtering for a portion of recorded motor tasks including continuous movement, velocity profiles, and filtering of horizontal and vertical components. A: An overlay of computer mouse x and y positions with the starting position and reach targets. Patients were instructed to move a computer mouse from the starting position (bottom center) to either the upper left or upper right corners of a computerized tablet, then return to the starting position. The target of each sequence was relayed verbally as a cue to begin movement. Movement sequences (outward reach and return) typically lasted 2–3 seconds with a brief pause at the target; however, only data recorded during outward reaching movement were used for analysis. Trials were marked by evaluating times at which velocity crossed a threshold. B: Overlaid

velocity profiles of trials in the up-left direction. C: Filtering of the vertical component of movement for each trial in the up-left direction. D: Filtering of the horizontal component of movement for each trial in the up-left direction. In both the vertical and horizontal cases, the *thick dark lines* indicate a single SD away from the average path. To be retained for further analysis, a trial must be ≥ 80% within the boundaries in both the horizontal and vertical components of movement. Retained trials are shown in *green*; discarded trials are shown in *dashed red*. Overall, 55% of trials in the patient in Case 1 and 56% of trials in Case 2 were retained for analysis.

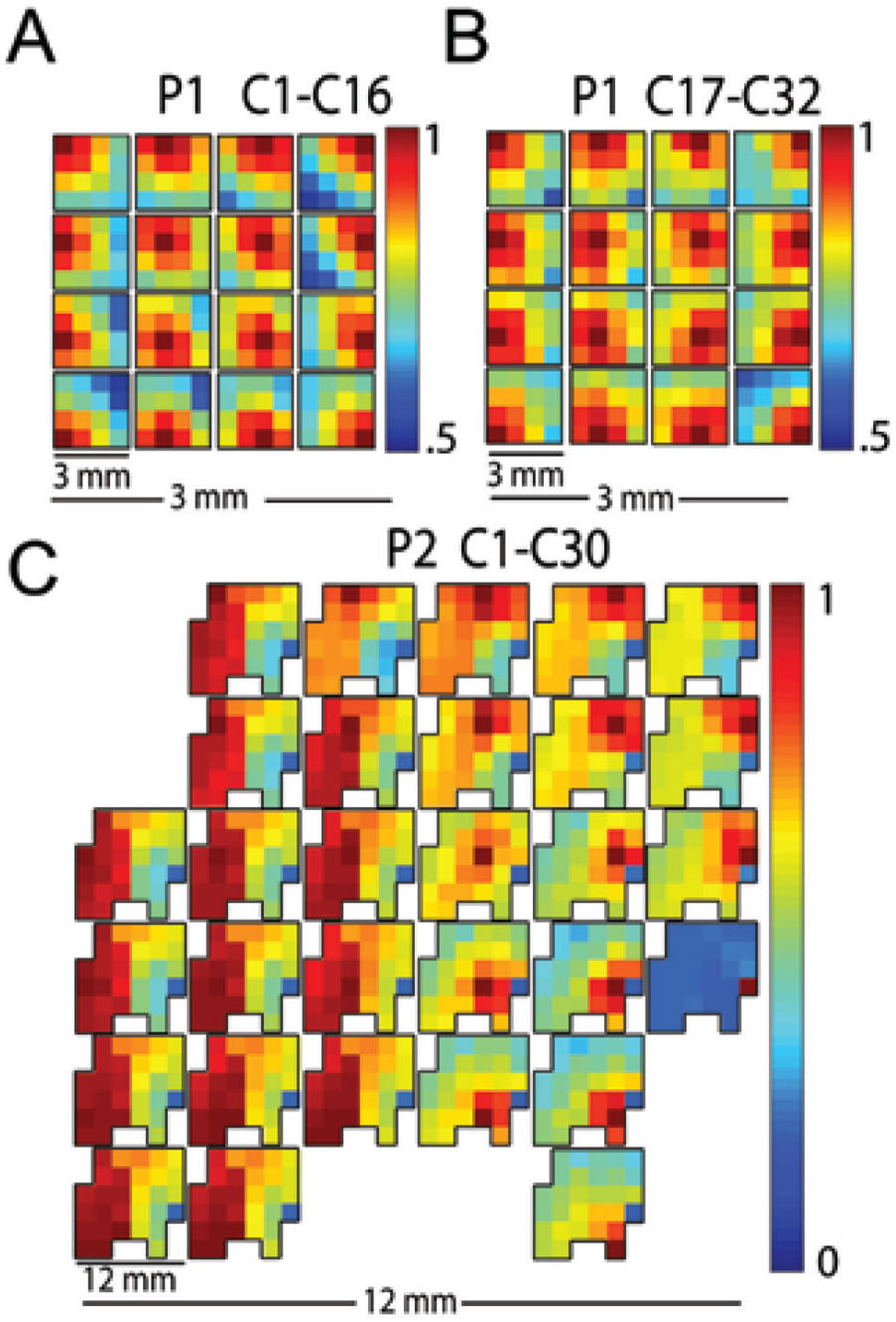

Fig. 3.

Gamma band (30–80 Hz) pairwise cross-correlations between each nonpenetrating microwire and all other microwires within an array. A: Array correlation, channels 1–16 (*orange wire* in Fig. 1) in the patient in Case 1 (P1). B: Array correlation in Case 1, channels 17–32 (*green wire* in Fig. 1.). C: Array correlation, 30 channels obtained in the patient in Case 2 (P2). The physical layouts of the devices in this figure are shown at 2 scales. At each location in the array, a miniature replica of the entire array indicates the pairwise cross-correlation of that nonpenetrating microwire with all other microwires in the array. The location itself is identifiable in the miniature replica by the dark red pixel showing the autocorrelation. Both arrays in Case 1 show an inverse relationship between correlation strength and distance. High

correlation between microwires in the anterior portion of Case 2, located over the hand area of primary motor cortex, contrasts with the decay seen in the posterior portion, which rested over the parietal cortex. The variation evident in correlation strength across arrays suggests that nonpenetrating microwire arrays can capture higher spatial resolution detail of neuronal signals than standard 5-mm-diameter ECoG electrodes that might rest over the same surface area. Note that the color scale is optimized to visually emphasize the correlation drop across a device.

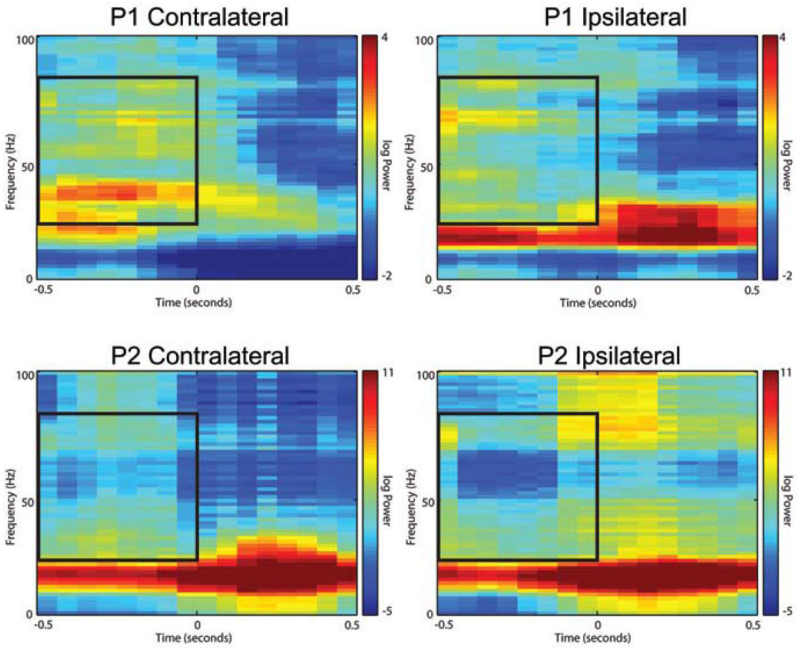

Fig. 4.

Spectrograms from a single nonpenetrating microwire for each patient demonstrating increased power in the gamma band during the planning phase for movement in the contralateral versus ipsilateral direction. These spectrograms are aligned at the 0-second tick to an outward reach movement. Recorded data from the nonpenetrating microwires were band-pass filtered to 5–150 Hz. Spectrograms were generated using the Chronux routines with a moving window of 250 msec and 50-msec step size; additionally, spectrograms were normalized to the average spectrum across time within the 1-sec window as described in the *Methods* section. Movement in the left column is toward the target contralateral to hemisphere in which the array was implanted; movement in the right column is toward the ipsilateral direction. *Inlaid boxed area* represents an outline of the gamma band for the planning stage evaluated in Fig. 7. Although only a single electrode is shown, the results are representative of most electrodes on each array.

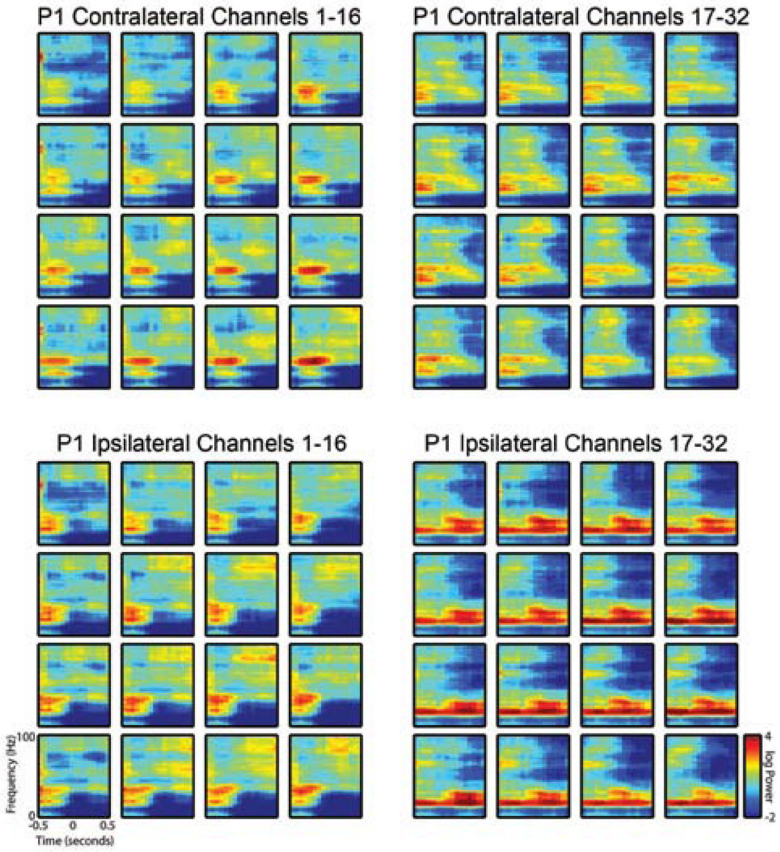

Fig. 5.

Spectrograms from all nonpenetrating microwires in the first patient (P1) demonstrating increased power in the gamma band during the planning phase for movement in the contralateral versus ipsilateral direction. Spectrograms were generated as described in the *Methods* section and the legend to Fig. 4. *Upper panels* show spectral content for movement toward the target contralateral to implantation hemisphere, and *lower panels* represent movement in the ipsilateral direction.

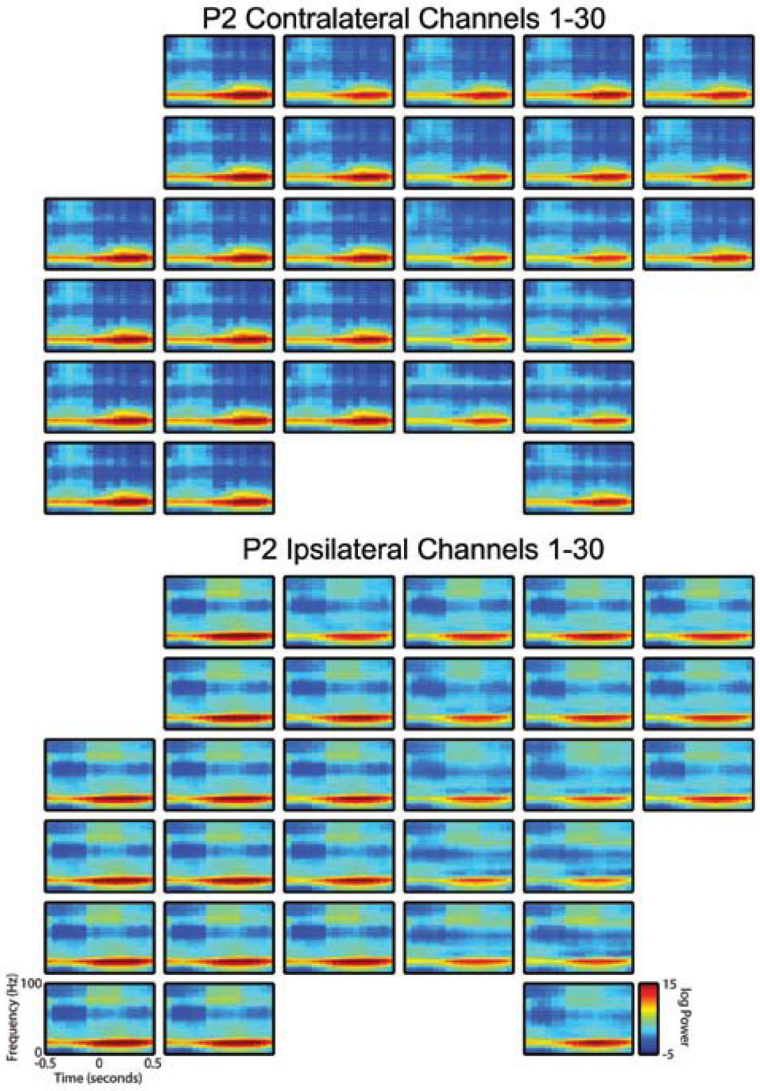

Fig. 6.

Spectrograms from all nonpenetrating microwires in the second patient (P2) demonstrating increased power in the gamma band during the planning phase for movement in the contralateral versus the ipsilateral direction. Spectrograms were generated as described in the *Methods* section and the legend to Fig. 4. *Upper panels* show spectral content for movement toward the target contralateral to implantation hemisphere; the *lower panels* represent movement toward the ipsilateral direction.

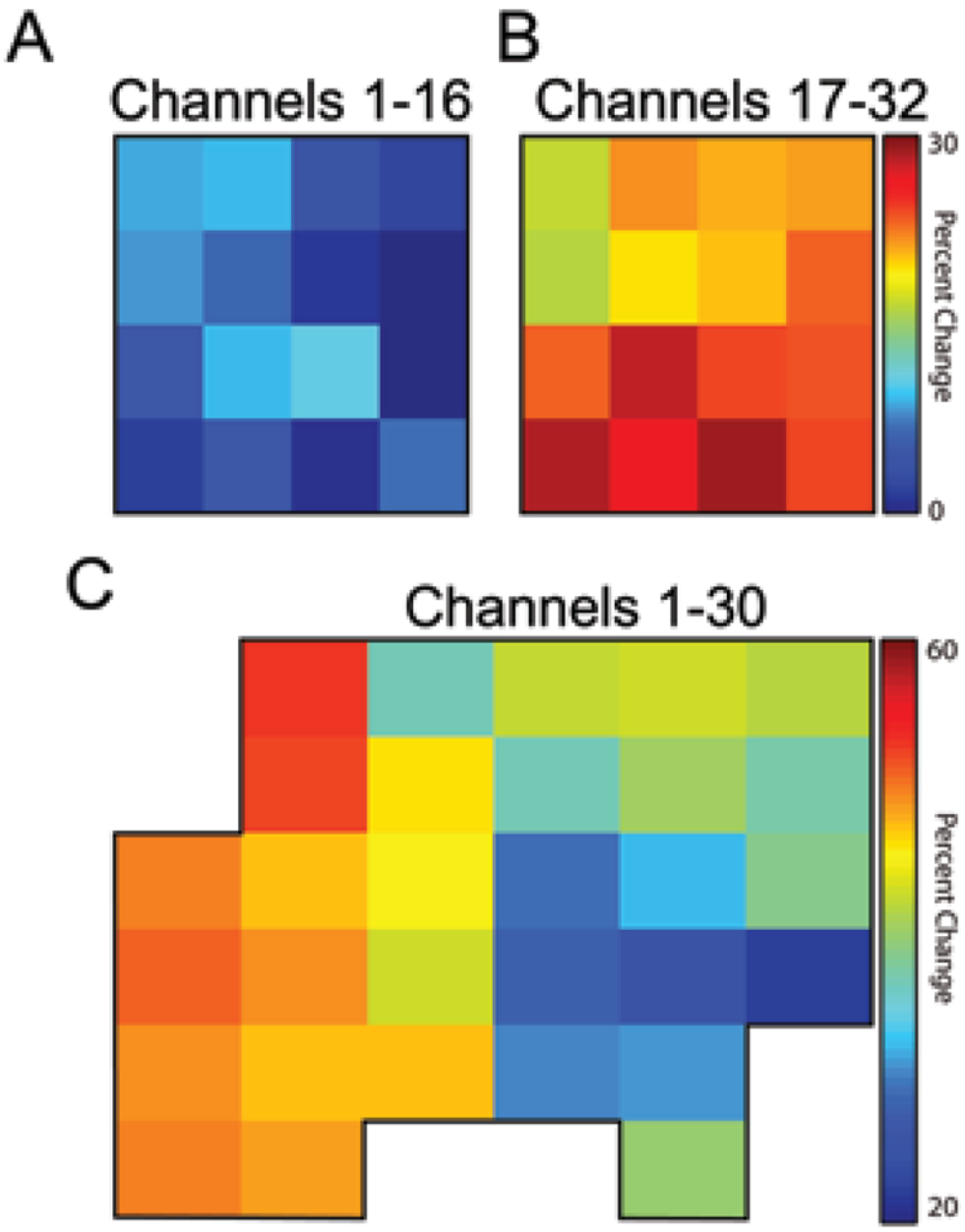

Fig. 7.

Plots showing, for each nonpenetrating microwire channel in each patient, the percent change in average gamma-band power during planning for movement in the contralateral direction over movement in the ipsilateral direction. After generating spectrograms for each channel as shown in Fig. 4, values for frequencies between 30 and 80 Hz and the full 500 msec before movement were averaged to a single value representative of the power over the entire gamma band during the movement planning phase. The difference between these mean values, normalized to the contralaterally directed mean values, is shown. In A and B, the percent change between contralaterally and ipsilaterally directed movement is shown for both electrode arrays implanted in the patient in Case 1. The disparity in magnitude of percent change between arrays is indicative of the underlying structure: channels 17–32 were located over the upper extremity primary motor cortex, whereas channels 1–16 were located more inferiorly along the precentral

gyrus. In C, the percent change between the contralateral and ipsilateral direction is shown for all 30 channels in the second patient. The patterns evident in C also correspond closely to the underlying anatomy as noted in the *Discussion* section.